

Nanostructured quasiperiodic surfaces: the origin of pentagonal hollows and their role in adsorption and nucleation processes

This article has been downloaded from IOPscience. Please scroll down to see the full text article.

2003 J. Phys.: Condens. Matter 15 S3113

(<http://iopscience.iop.org/0953-8984/15/42/009>)

View [the table of contents for this issue](#), or go to the [journal homepage](#) for more

Download details:

IP Address: 171.66.16.125

The article was downloaded on 19/05/2010 at 15:21

Please note that [terms and conditions apply](#).

Nanostructured quasiperiodic surfaces: the origin of pentagonal hollows and their role in adsorption and nucleation processes

J Ledieu and R McGrath

Surface Science Research Centre and Department of Physics, The University of Liverpool,
Liverpool L69 3BX, UK

E-mail: mcgrath@liv.ac.uk

Received 2 May 2003

Published 10 October 2003

Online at stacks.iop.org/JPhysCM/15/S3113

Abstract

Pentagonal hollows, which are imaged as dark five-fold stars, form the dominant structural motif in scanning tunnelling microscopy (STM) measurements of the five-fold surfaces of icosahedral quasicrystals. Recent progress in the understanding of these surfaces has led to a thorough understanding of these entities; we illustrate how they may be considered as truncations of the basic building blocks (i.e. Bergman clusters) of the bulk structure. The use of these pentagonal hollows as adsorption and nucleation sites is demonstrated using STM images of their filling during scanning of the clean Al–Pd–Mn surface and in the adsorption of C₆₀ molecules and copper atoms on Al–Pd–Mn and of aluminium atoms on Al–Cu–Fe.

1. Introduction

One of the main goals in nanoscience is to find ways to tailor atomic arrangements on surfaces. Consequently, a huge effort has been put into understanding the formation and properties of nanoscale atomic structures [1]. A prominent example is the ‘quantum corral’ created by Eigler *et al* [2] by atomic manipulation using a scanning tunnelling microscopy (STM) tip. An alternative route to nanostructure formation is through self-assembly of atoms or molecules. This has the obvious advantage of creating identical atomic patterns rapidly and over a macroscopic scale. This is the path we have chosen in attempting to generate novel symmetry nanostructure formations, using quasicrystal surfaces as templates.

Quasicrystals, first discovered in 1982 [3], are bi- and tri-metallic ternary alloys. They lack translational symmetry, but possess long range order. There are several different structural families of quasicrystals; in this paper we will concentrate on the Al₇₀Pd₂₁Mn₉ and Al₆₁Cu₂₅Fe₁₄ quasicrystals. These are among the best understood quasicrystals as successful models of the bulk structure have been obtained. They have the symmetries of an icosahedron

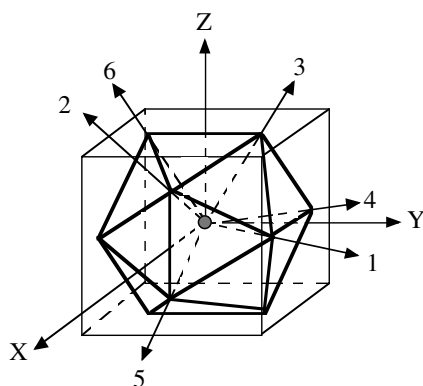


Figure 1. Regular icosahedron showing six five-fold axes of rotation (after [4]).

(one of the five platonic solids, see figure 1) which include three-fold, two-fold and five-fold axes of rotation. The surfaces of these quasicrystals are now also reasonably well understood. In this paper we will concentrate on the surfaces which are perpendicular to a five-fold axis of rotation of the bulk material.

Two topographies are obtained for these surfaces by ultra high vacuum (UHV) sputter/anneal techniques: a rough surface which has been dubbed the ‘clustered phase’ and a terrace-like surface called the ‘flat terraced phase’. The first scanning STM images obtained on the ‘flat terraced phase’ of the $\text{Al}_{70}\text{Pd}_{21}\text{Mn}_9$ surface revealed a terraced-like topography with two step heights following a Fibonacci sequence [5]. On images of the terraces a dominant motif is the appearance of dark five-fold stars of edge length $4.8 \pm 0.2 \text{ \AA}$. In this paper we review the comparison with the bulk model and emphasize the origin of these pentagonal hollows as arising from the dissection of Bergman clusters which can be regarded as basic building blocks of the bulk structure. We then highlight the role of these pentagonal hollows in the adsorption process by showing examples of the adsorption of different atomic and molecular species.

The organization of the paper is as follows: we first show STM data of the clean Al–Pd–Mn surface. We then compare this data with the predictions of the bulk model, confirming the predicted variation of the density of the pentagonal hollows [6] and identifying the origin of the pentagonal hollows. We show the filling of a pentagonal hollow during scanning of the surface which confirms the nature of these hollows and places experimental limits on their depth. We discuss the role of the pentagonal hollows as atomic and molecular adsorption/nucleation sites.

2. Clean surface studies: the origin of the dark five-fold stars

2.1. STM observations

For single crystal metal surfaces good quality (low energy electron diffraction) LEED patterns (sharp diffraction spots with a low background) are associated with well-prepared, atomically flat surfaces. For quasicrystals this is not as straightforward to judge. A reasonable quality five-fold LEED pattern can be obtained within an hour and subsequent investigation by STM demonstrates a rough corrugation on the surface. To produce the flat-terraced phase requires several cycles of sputtering and annealing: typically a total of 5 h Ar^+ sputtering at grazing angle and 12 h annealing to 970 K by e-beam heating.

After this surface treatment sharp diffraction spots are present from beam energies of 10 eV up to 350 eV (see figure 2(A)). STM measurements were taken with Omicron systems, all at room temperature. These images show large flat terraces with a typical width of $0.3 \mu\text{m}$ for a length of the order of several micrometres (see [7]). At higher magnification atomic resolution is obtained on each terrace (see e.g. figure 2(B)). A fast fourier transform (FFT) of figure 2(B) demonstrates the quasicrystallinity of the image (see figure 2(C)). The surface is atomically flat with a surface corrugation of 0.27 \AA . Sequences of atomically resolved STM images (not shown) were recorded from terrace to terrace by shifting the area frame incrementally across the surface. Two step heights, 4.1 and 6.6 \AA following the Fibonacci sequence, are present at the surface of the $\text{Al}_{70}\text{Pd}_{21}\text{Mn}_9$ quasicrystal [8].

The dark five-fold stars form a dominant motif. Figure 3 shows a close-up of one in a three-dimensional representation. It is apparent that the five-fold appearance of the hollows arises from the surrounding five protrusions, and that these dark five-fold stars are in fact pentagonal hollows in the surface. The following observations may be made regarding these pentagonal hollows:

- (i) The hollows have edge length of 4.8 \AA .
- (ii) The orientation of the hollows is the same direction within each terrace, and across all terraces on the surface. This has been checked over several micrometres. This is consistent with the five-fold symmetry exhibited by the LEED pattern shown in figure 2(A).
- (iii) The density of the hollows varies from terrace to terrace. Figure 4 shows data from two adjacent terraces: the density of five-fold hollow sites is estimated to be about three times less on figure 2(A) than on figure 2(B).
- (iv) A lower limit can be placed on the depth of the hollows. STM relies on the measurement of the tunnelling current which is proportional to the electron local density of states (LDOS) at E_F . Therefore it is non-trivial to judge the real depth of the hollows, as the tip does not probe the true depth due to loss of tunnelling within the hollows. However the minimum depth of the hollows is estimated at $1.2 \pm 0.2 \text{ \AA}$.
- (v) The five-fold surface of Al–Pd–Mn has been described as a ‘Fibonacci pentagrid’ [5]. This reflects the fact that structural entities of this aperiodic material are related by the mathematics of the Fibonacci sequence [9]. This means that the spacing between similar planes of the bulk structure have not one but two dominant spacings, and this is reflected in the two step heights observed on the surface [5]. Furthermore, on any five-fold terrace, arrangements of structural elements also show Fibonacci interrelationships. This is illustrated in figure 5 which shows a high resolution image of the five-fold surface of Al–Pd–Mn. White lines drawn on the figure join identical positions on the dark five-fold stars; the separations between the lines are of two lengths $L = 7.4 \pm 0.2 \text{ \AA}$ and $S = 4.6 \pm 0.2 \text{ \AA}$, whose ratio is within experimental error equal to the golden mean τ ; (τ is the irrational number expected for the ratio of the two basic units of the Fibonacci sequence ($\tau = (\sqrt{5} + 1)/2 = 1.618\dots$)). The arrangement of these line separations (reading from top to bottom) *LSLLSLSL* forms a segment of the Fibonacci sequence. Furthermore, along any line, the positions of the five-fold stars are related by powers τ . These relationships are used in section 3.2 to help identify the adsorption site of C_{60} molecules on the surface.

2.2. Comparison with the bulk model

How do these measurements compare with the bulk model? We first give a brief description of the salient features of this model. The model consists of a 3D quasiperiodic tiling (which

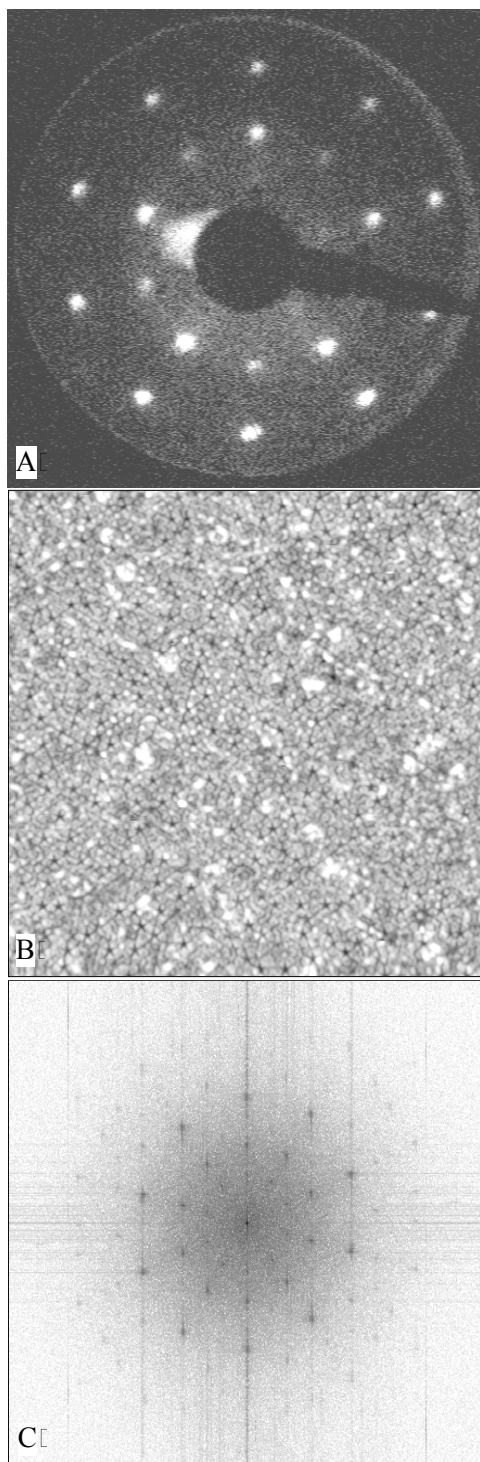


Figure 2. (A) Five-fold symmetric LEED pattern of the flat terraced phase of the five-fold surface of Al-Pd-Mn obtained at 12 eV. (B) $400 \text{ \AA} \times 400 \text{ \AA}$ high resolution image of this surface. (C) FFT of the STM image in (B).

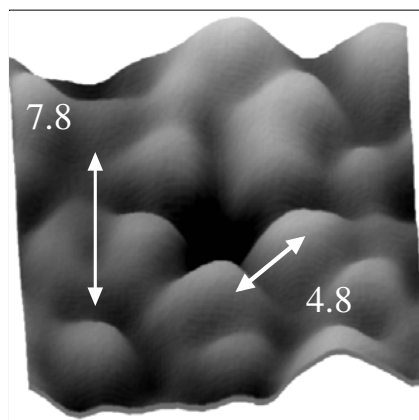


Figure 3. $20 \text{ \AA} \times 20 \text{ \AA}$ pseudo 3D image of a dark five-fold star on the surface of Al-Pd-Mn showing the formation of a pentagonal hollow by the surrounding areas of high contrast.

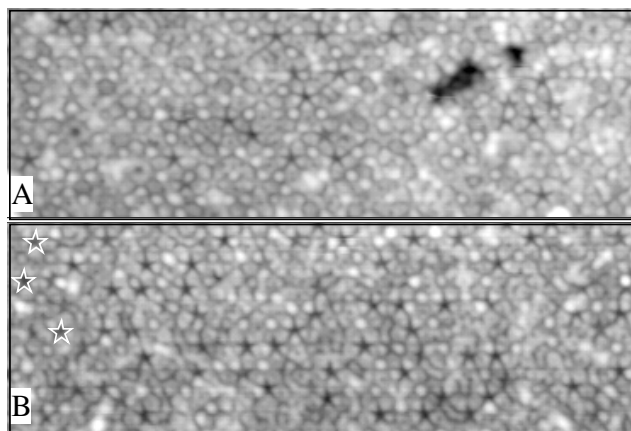


Figure 4. (A), (B) $300 \text{ \AA} \times 100 \text{ \AA}$ atomic resolution images of the five-fold surface of Al-Pd-Mn showing the different density distribution of holes on consecutive terraces. Three pentagonal hollows are outlined on (B).

is derived from a 6D hypercubic lattice [10–12]). The vertices of this tiling are embedded within planes perpendicular to the five-fold axes of an icosahedron (parallel to the surface studied here). The relative position of those planes in the model obeys the Fibonacci sequence (aperiodically stacked). These vertices are then decorated with Bergman clusters to provide atomic positions. Bergman clusters can be viewed as basic buildings blocks within the model. A 3D representation of a Bergman cluster is shown on figure 6(A). It consists of 33 atoms distributed as follows: 1 central atom, 12 atoms decorating an icosahedron for the intermediate shell and 20 atoms distributed on a dodecahedron as the external shell.

Although each layer within the model is chemically and structurally different, recent workers have come to the same conclusion [6, 7, 13–18]: the fivefold surfaces of the icosahedral quasicrystals are ‘laterally’ bulk-terminated and almost chemically/structurally identical to each other. This identification then leads to the explanation of the observations regarding the pentagonal hollows presented in 2.1. In particular:

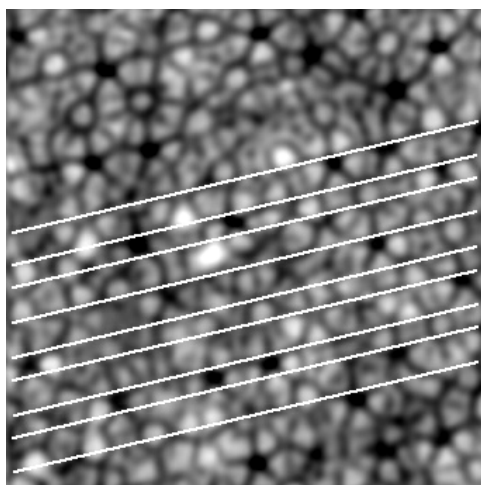


Figure 5. $100 \text{ \AA} \times 100 \text{ \AA}$ atomic resolution image of the five-fold surface of Al-Pd-Mn. White lines having two distinct spacings L and S join similar points on the five-fold stars; the spacings of these lines (reading from top to bottom) follow a pattern $LSLLSLSL$ which is consistent with terms of the Fibonacci sequence.

- (i) The appearance of the pentagonal hollows can be related to the dissection of Bergman clusters at a particular section during the annealing process (see figure 6(B)) [7]. A cut through a Bergman cluster at a precise height generates a pentagon of edge length 4.8 \AA consistent with measurements obtained from STM images.
- (ii) The model predicts that the hollows should have the same orientation everywhere on the surface, in agreement with the observations.
- (iii) The variation of the density of hollows on the terraces is what is expected for the bulk model. This has been demonstrated recently using a tiling approach where it was found that the experimentally derived Penrose tiling of the surfaces agrees both in form and in scale with the predictions of the bulk geometric model. Surface planes are understood as cuts through Bergman layers of different density. From the number of five-fold hollow sites shown per terrace one can deduce the density of the layer dissected by the plane: more pentagonal hollows correspond to more dissected Bergman clusters. These aspects are extensively discussed in a recent publication [8] and the reader is referred to this paper for further details.
- (iv) A theoretical estimate of the depth of the pentagonal hollows is possible. In the case of the $\text{Al}_{70}\text{Pd}_{21}\text{Mn}_9$ planes analysed in previous work [7], five-fold hollow sites appear as deep as 1.99 \AA .

Furthermore the two step heights observed can be explained as arising from cuts through the Bergman clusters: the height of the cluster along the five-fold axes is equal to 6.6 \AA .

Finally, a comment can be made about cluster stability. Intact clusters have been observed after cleavage along the five-fold axis of $i\text{-Al}_{70}\text{Pd}_{21}\text{Mn}_9$, which has been explained by crack propagation along zones of lower strength [19]. However the long annealing process breaks the clusters and one can regard them as geometric building blocks for the bulk model rather than energetically stable entities [6, 7, 12].

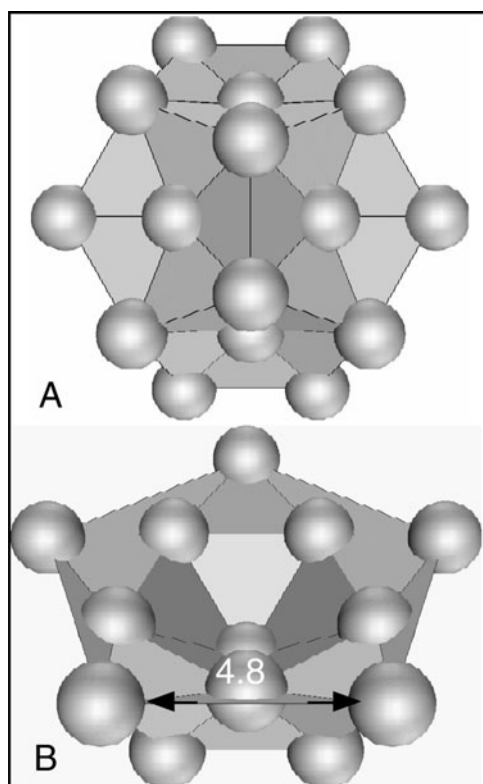


Figure 6. (A) 3D representation of a Bergman cluster. (B) Dissected Bergman polytope. A pentagonal hollow of edge length equal to 4.8 Å is created and corresponds to those observed on STM images. (Image courtesy of G Kasner.)

3. Pentagonal hollows as adsorption and nucleation sites

The depth and width of the pentagonal hollows immediately suggests that they can act as adsorption sites: an atom or molecule can physically fit within such a hollow. If one could fill such sites and none others on these surfaces with adsorbates, a 2D quasiperiodic array should emerge. In this section we present evidence that these sites are indeed of great importance in the adsorption and nucleation processes. We first show the filling of such sites during scanning of the clean surface, and then describe three adsorption systems where these sites are preferentially filled.

3.1. Filling of pentagonal hollows during scanning of the clean surface

Tip induced motion has been observed in several studies specially when scanning adsorbates and molecules/atoms on a substrate. Recording several scans of the same area with identical or different tunnelling parameters sometimes allows the tip to move or drop atoms on the surface. Figures 7(A), (B) represents the same region during successive scans. The five-fold hollow site shown by the arrow has been filled by a single atom. This observation highlights the potential of these sites as adsorption and nucleation centres.

It has been demonstrated that under certain tunnelling conditions the STM may image some atoms as depressions; an example is the case of oxygen adsorption on Al(111) where

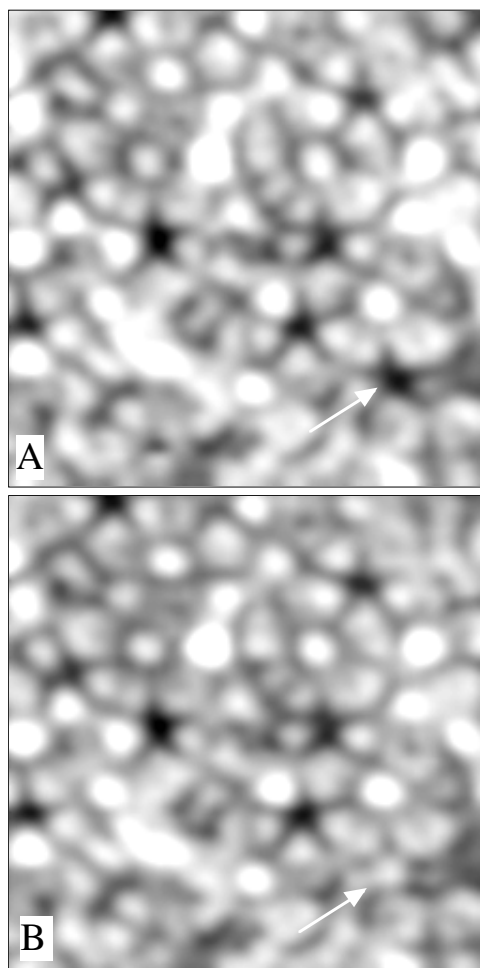


Figure 7. (A) and (B) $60 \text{ \AA} \times 60 \text{ \AA}$ high resolution images of the clean surface of Al-Pd-Mn. The arrow points to a five-fold hollow site being filled after several scans of the same area.

oxygen atoms appear as hollows [20]. The hole-filling demonstrated here is further evidence that these pentagonal hollows are true depressions on the surface, and not an artefact such as that described above. We can also exclude the hypothesis that the effect shown in figure 7 is merely a change in contrast caused by exchange of atoms between the tip and the surface. Such an exchange process would cause all subsequent hollows scanned to appear as filled, and would affect the contrast across the entire image. This is clearly not the case here.

3.2. C_{60} adsorption on Al-Pd-Mn

C_{60} molecules have a cage diameter of $\sim 7.1 \text{ \AA}$ which is comparable to the height of the pentagonal hollows¹ ($\sim 7.8 \text{ \AA}$). Based on this geometric consideration C_{60} molecules appear to be good candidates for decorating these sites. At low coverages ($\sim 0.065 \text{ ML}$), C_{60} molecules adsorb in an isotropic manner without preferential decoration of step edges or

¹ The height of a pentagon or pentagram is defined as the distance from its base to the opposite apex.

island formation [21]. As the coverage is increased the density of adsorbates increases. No hexagonal ordering is observed within the adsorbates and the layer, although almost complete, is still disordered. The LEED pattern fades and then vanishes as the coverage is increased.

As described in section 2.1, and illustrated in figure 5, the pentagonal hollow sites are aligned along a so-called ‘Fibonacci pentagrid’ on the quasicrystal surface, and the distances between such hollow sites are subject to τ -scaling relationships, i.e. if the distances between two hollows is multiplied by τ or powers of τ then the resulting distance locates other such hollows along the same line.

With deposition of C_{60} on the quasicrystal surface, the STM resolution of the substrate diminishes. This is mainly due to the height of the adsorbates. However at low coverage (~ 0.065 ML) the pentagonal hollows are still visible. This allows us to locate where the next hollows should appear. By careful examination, it is confirmed that C_{60} molecules are adsorbed in those hollow sites. Adsorbates are aligned along the same directions as the hollows and a τ -scaling relationship between intermolecular distances can be recognized. This is illustrated in figure 8(a); the intermolecular distances are related by

$$[AE] = \tau[AD] = \tau^2[AC] = \tau^3[AB] \quad (1)$$

and

$$[EH] = \tau[EG] = \tau^3[EF]. \quad (2)$$

Although plot profiles across C_{60} (height $< \sim 7$ Å) suggest that adsorbates are embedded within the top layer (sitting in the hollows) this feature could be linked to a charge transfer from the adsorbates to the surface layer reducing the LDOS of the C_{60} and therefore reducing their apparent heights.

At higher coverage τ -scaling relationships between C_{60} molecule positions are lost as multiple sites are occupied. This is shown in figure 8(b). This is explained by the decrease in the number of five-fold hollow sites available due to filling, by site blocking due to the large cage diameter of the adsorbates [21], and by the consequent reduced diffusivity of the C_{60} molecules on the terraces.

3.3. Copper adsorption on Al–Pd–Mn

The second adsorption system is that of Cu atoms deposited on the flat-terraced phase of Al–Pd–Mn. Just as for the C_{60} /Al–Pd–Mn system different coverages were studied. Only the low coverage (0.08 ML) case is presented here.

Prior to dosing the clean surface is investigated by LEED, AES and STM in order to check the quasicrystallinity of the top layers. STM scans obtained after adsorption of 0.08 ML of Cu reveal island formation (see figure 9(a)). A FFT is shown (bottom left corner) and exhibits a ring of ten spots as expected for a quasicrystal surface. As the dosage is increased islands start to coalesce to form an almost complete monolayer.

Figures 9(b) and (c) correspond to two regions from figure 9(a) (white squares). The lack of dark five-fold stars on these images is striking. The arrows on figure 9(b) point to several pentagonal hollows whose centres are filled by a single atom. The size of those sites is consistent with the pentagonal hollows previously described. On figure 9(c) white arrows point to a number of pentagonal hollows which are still empty.

Because empty and filled five-fold sites are imaged on the same STM scan, the lack of hollows in figure 9 cannot be explained by a loss of substrate resolution. It is therefore reasonable to suggest Cu atoms populate the five-fold hollows sites before nucleation of islands takes place. It is also probable that once ‘buried’ in those positions Cu adatoms act as nucleation sites for island growth.

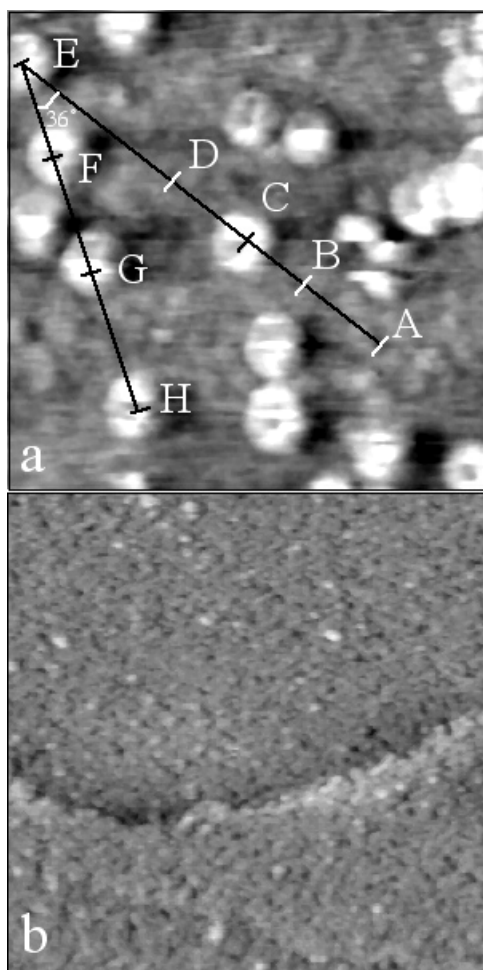


Figure 8. (a) $150 \text{ \AA} \times 150 \text{ \AA}$ image of the Al-Pd-Mn surface at a C_{60} coverage of 0.065 ML. (b) $900 \text{ \AA} \times 900 \text{ \AA}$ image of the Al-Pd-Mn surface at a C_{60} coverage of 1 ML.

3.4. Aluminium adsorption on Al-Cu-Fe

Finally aluminium adsorption on the five-fold icosahedral $Al_{61}Cu_{20}Fe_{14}$ quasicrystalline surface has been studied [22]. Although the material is different, the surface layer is structurally very similar. Both surfaces are also aluminium rich. Figures 10(a) and (b) represent two planes from Al-Pd-Mn and Al-Cu-Fe bulk models respectively. The surfaces of both samples are bulk-terminated. (Planes shown on figures 10(a) and (b) can be considered as good representations of surface terminations [16].) Identical hollow sites are present on both quasicrystal surfaces. This is outlined by grey pentagons on figures 10(a), (b). The pentagonal hollow edge lengths are equal theoretically to 4.8 \AA for Al-Pd-Mn and 4.7 \AA for Al-Cu-Fe.

Figure 10(c) represents an STM image of the Al-Cu-Fe surface (black part) dosed with 0.04 ML of Al atoms (orange/grey stars). The substrate is well resolved by STM but it has been darkened here to outline the adsorbates. At low coverage aluminium atoms diffuse across the surface and nucleate to form clusters, which have been dubbed 'starfish' due to their five-fold symmetry (see figure 10(c)). The formation of such starfish is highly reproducible. It is also

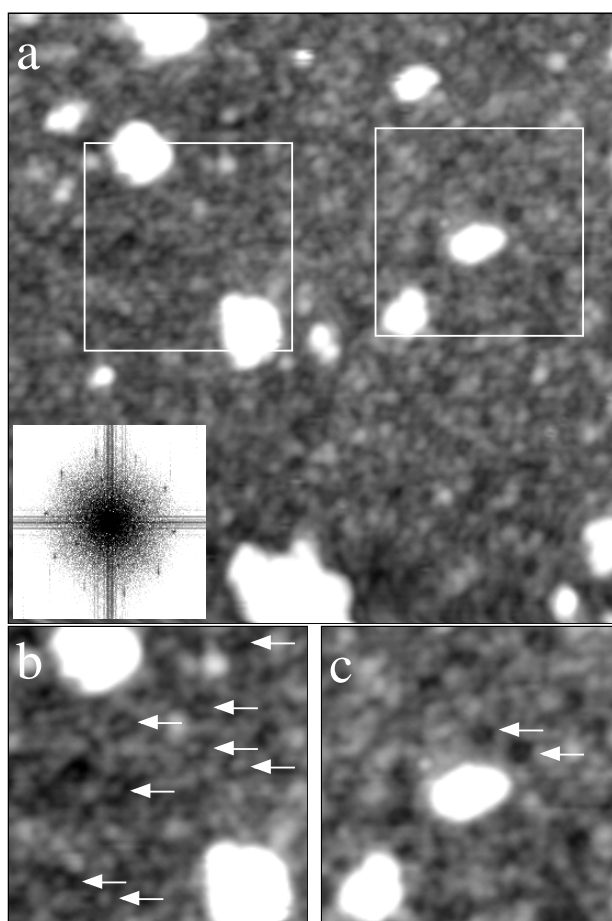


Figure 9. (a) $225 \text{ \AA} \times 225 \text{ \AA}$ STM image of a Al-Pd-Mn surface dosed with 0.08 ML of Cu. A FFT has been calculated and reveals the five-fold symmetry of the image obtained. (b), (c) $80 \text{ \AA} \times 80 \text{ \AA}$ regions taken from (a). Arrows on (b) point to five-fold hollow sites being occupied while arrows on (c) indicate the remaining unoccupied ones.

independent of the deposition flux which is a good indication of inhomogeneous nucleation. Higher magnification STM images indicate that the starfish legs are composed of five well resolved atoms. All starfish recorded at the surface show a similar height (monatomic) and size (edge length equal to $\sim 5.1 \text{ \AA}$). They also point in the same direction from terrace to terrace.

The substrate structure is still well resolved by STM for 0.04 ML coverage and this allows us to locate the position of the starfish on the surface [22]. From the uniformity in size and orientation of the starfish across the surface, the nucleation site has to be identical within and among terraces. As described in [22], only the five-fold hollow sites (see figure 10(b)) match these requirements. The model proposed is that aluminium atoms arriving at the surface of the Al-Cu-Fe sample diffuse into these hollows and, like Cu atoms in section 3.3, act as a nucleation site for the growth of the starfish. Therefore each starfish is composed of five external atoms plus one in the centre.

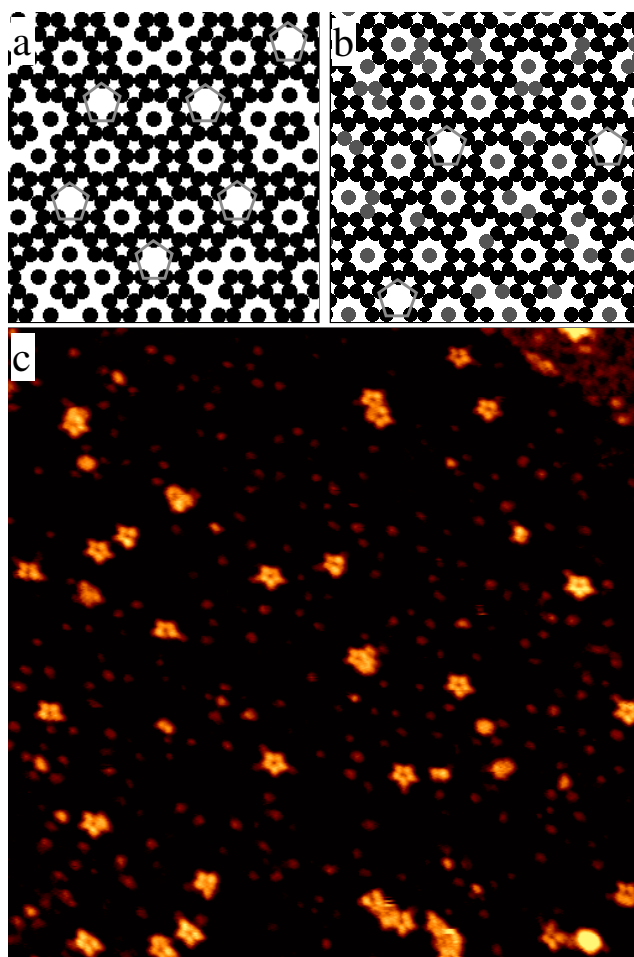


Figure 10. (a), (b) $60 \text{ \AA} \times 60 \text{ \AA}$ planes from Al–Pd–Mn (black: Al) (a) and Al–Cu–Fe models (black: Al, grey: Fe) (b). Grey pentagons outline the five-fold hollow sites of the two surface planes [23]. (c) $420 \text{ \AA} \times 420 \text{ \AA}$ STM image of an Al–Cu–Fe surface dosed with 0.04 ML of Al adatoms. The contrast of the STM image has been saturated for clarity (black: substrate, orange (grey): starfish). Reprinted from [22] with permission from Elsevier.

(This figure is in colour only in the electronic version)

4. Summary

We have illustrated that the pentagonal hollows observed on the five-fold surfaces of icosahedral quasicrystals arise from the dissection of Bergman clusters as the surface is formed during the annealing process. The filling of these pentagonal hollows has been observed with STM and their role as adsorption and nucleation sites has been highlighted and clarified.

Acknowledgments

The EPSRC is acknowledged for funding. We acknowledge the contributions of several co-authors on several of the papers cited in this paper. M de Boissieu, Z Shen and P A Thiel are thanked for the use of the software used to generate the two-dimensional atomic planes.

References

- [1] Moriarty P 2001 *Rep. Prog. Phys.* **64** 297
- [2] Crommie M F, Lutz C P and Eigler D M 1993 *Science* **262** 218
- [3] Shechtman D, Blech I, Gratias D and Cahn J W 1984 *Phys. Rev. Lett.* **53** 1951
- [4] Janot C 1994 *Quasicrystals, A Primer* 2nd edn (Oxford: Oxford Science Publications) p 69
- [5] Schaub T M, Bürgler D E, Güntherodt H-J and Suck J-B 1994 *Phys. Rev. Lett.* **73** 1255
- [6] Kasner G, Papadopolos Z, Kramer P and Bürgler D E 1999 *Phys. Rev. B* **60** 3899
- [7] Ledieu J, Dhanak V R, Diehl R D, Lograsso T A, Delaney D W and McGrath R 2002 *Surf. Sci.* **512** 77
- [8] Papadopolos Z, Kasner G, Ledieu J, Cox E J, Diehl R D, Richardson N V, Chen Q, Lograsso T A, Ross A R and McGrath R 2002 *Phys. Rev. B* **66** 184207
- [9] Garland T H 1987 *Fascinating Fibonacci: Mystery and Magic in Numbers* (USA: Dale Seymour Publications)
- [10] Katz A and Gratias D 1995 *Proc. 5th Int. Conf. on Quasicrystals* ed C Janot and R Mosseri (Singapore: World Scientific) p 164
- [11] Elser V 1996 *Phil. Mag. B* **73** 641
- [12] Papadopolos Z, Kramer P and Liebermeister W 1998 *Proc. Int. Conf. on Aperiodic Crystals, Aperiodic 1997* ed M de Boissieu, J-L Verger-Gaugry and R Currant (Singapore: World Scientific) p 173
- [13] Gierer M, Van Hove M A, Goldman A I, Shen Z, Chang S-L, Pinhero P J, Jenks C J, Anderegg J W, Zhang C-M and Thiel P A 1998 *Phys. Rev. B* **57** 7628
- [14] Papadopolos Z, Kramer P, Kasner G and Bürgler D E 1999 *Mater. Res. Soc. Symp. Proc.* **553** 231
- [15] Shen Z, Stoldt C R, Jenks C J, Lograsso T A and Thiel P A 1999 *Phys. Rev. B* **60** 14688
- [16] Cai T, Fournée V, Ross A R, Lograsso T A and Thiel P A 2002 *Phys. Rev. B* **65** 140202
- [17] Ledieu J, Munz A W, Parker T M, McGrath R, Diehl R D, Delaney D W and Lograsso T A 1999 *Surf. Sci.* **433–435** 665
- [18] Barbier L, Le Floc'h D, Calvayrac Y and Gratias D 2002 *Phys. Rev. Lett.* **88** 085506
- [19] Ebert Ph, Feuerbacher M, Tamura N, Wollgarten M and Urban K 1996 *Phys. Rev. Lett.* **18** 3827
- [20] Winterlin J, Brune H, Höfer H and Behm R J 1988 *Appl. Phys. A* **47** 99
- [21] Ledieu J, Muryn C A, Thornton G, Diehl R D, Lograsso T A, Delaney D W and McGrath R 2001 *Surf. Sci.* **472** 89
- [22] Cai T, Ledieu J, Fournée V, Lograsso T A, Ross A R, McGrath R and Thiel P A 2003 *Surf. Sci.* **526** 115
- [23] Boudard M, de Boissieu M, Janot C, Heger G, Beeli C, Nissen H-U, Vincent H, Ibberson R, Audier M and Dubois J M 1992 *J. Phys.: Condens. Matter* **4** 10149